Wave Propagation in Functionally Graded Material Bar Due to Collision

Tadaharu Adachi and Masahiro Higuchi

Abstract We mathematically analyzed wave propagations in functionally graded material (FGM) bars collided by a homogeneous bar on the basis of Laplace transformation and calculated by using numerical Laplace transformation and its inversion. Young's modulus in the FGM bar was assumed to be proportional to the square of its density, which was similar to foam materials. Finally in the FG bar with increasing modulus from the impact end to the fixed end, much larger compressive stress and even large tensile stress occurred near the fixed end. In the FG bar with decreasing modulus from the impact end, the stress history varied moder-ately however large tensile stress occurred.

1 Introduction

Functionally graded materials (FGMs) [1, 2] are suggested to be applied materials for impact energy absorption [1–6]. Longitudinal impact response of the FGMs must be clarified to investigate the impact energy absorption characteristics of FGMs.

Longitudinal responses of FGMs have been analyzed by several researchers until now. Chiu and Erdogan [7] analyzed FGM's longitudinal impact problems. The stress history of FGM has been analyzed by Bruck [8], and more recently Abu-Alshaikh and Kokluce [9] showed that elastic wave propagation in FGM could be analyzed by using an approximate model expressed as a laminate of

T. Adachi (✉)
Department of Mechanical Engineering, Toyohashi University of Technology, 1-1 Hibarigaoka, Tempaku, Toyohashi, 441-8580, Japan
e-mail: adachi@me.tut.ac.jp

M. Higuchi
School of Mechanical Engineering, Kanazawa University, Kakuma-machi, Kanazawa, 920–1192, Japan
e-mail: higuchi-m@se.kanazawa-u.ac.jp

Alexander K. Belyaev et al. (eds.), *Mechanics and Model-Based Control of Advanced Engineering Systems*, DOI 10.1007/978-3-7091-1571-8_1,

thin homogeneous plates. Cui [6] evaluated energy absorption characteristics of FGMs by using a laminated model, as well. Kiernan et al. [10] simulated split Hopkinson bar tests for FGMs by finite element analysis. Han et al. [11] and Santare et al. [12] considered finite elements in a finite element analysis of elastic wave propagation in FGM. Samadhiya et al. [13] used a laminate model to perform a spectral analysis of FGM vibration. Berezovski et al. [14] analyzed dynamic stress in FGMs that had non-uniform dispersion of particles. Liu et al. [15] investigated how to identify the distribution of material properties in FGMs on the basis of elastic wave propagation. The authors recently analyzed the longitudinal impact problem of FGMs mathematically and clarified that the distribution slope of the material properties was significant for understanding stress histories generated in FGMs [16, 17]. The longitudinal impact problems of FGMs have previously been analyzed and considered, as outlined above. In order to clarify FGM impact energy absorption from the viewpoint of impact response, we need to analyze the problem of an FGM colliding with an impactor and consider the relation between the distribution of material properties and the impact response of the FGM. This FGM collision problem has not yet been analyzed.

In the present study, wave propagation in an FGM bar collided with an impactor is analyzed to determine the suitability of FGM as a material for energy absorption. The impact load and stress problems in the FGM bar are solved mathematically by using Laplace transformation. Numerical Laplace transformation and its inversion are formulated and applied to compute the solutions. A material model of the FG bar is assumed to have foam material characteristics.

2 Analysis

2.1 Analytical Collision Model

We analyze wave propagation in an FGM bar subjected to collision with a homogeneous impact bar, as shown in Fig. 1. An FGM bar with a length of L is collided at a velocity of V_0 with an impact bar with a length of L_I. To simplify the problem, the cross sectional areas of both bars are the same and the materials of both bars are linearly elastic in the analysis. The density and elastic modulus in the FGM bar are distributed along the axial coordinate, x. The Young's modulus, $E(x)$ is assumed to be proportional to the square of the density, $\rho(x)$ [18, 19] as

$$\rho(x) = \rho_0 \varphi(x)\,,\ E(x) = E_0(\varphi(x))^2, \tag{1}$$

where $\varphi(x)$ is the shape function of the distribution. The shape function is assumed to be

$$\varphi(x) = \Phi_1 \left(\frac{x}{L} + \Phi_0 \right)^2, \tag{2}$$

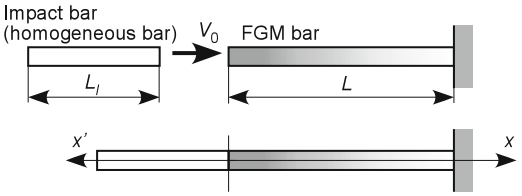

Fig. 1 Collision problem of FGM bar

where Φ_1 and Φ_0 are coefficients determined from the distribution in the FGM bar. The density and Young's modulus in the impact bar are ρ_I and E_I.

The stress-strain relation of the FGM is expressed by Hooke's law.

$$\sigma(x,t) = E(x)\varepsilon(x,t), \tag{3}$$

where σ, ε and t are stress, strain and time, respectively. The strain in the FGM bar is axial displacement, u differentiated by axial coordinate, x. The displacement of the FGM bar at the impacted tip, $U(t)$ must coincide with that of the impact bar at the tip, $U_I(t)$ during contact between the bars if local deformation near the contact area of both bars is neglected.

$$U(t) = V_0 t - U_I(t). \tag{4}$$

The displacement of both bars at the tip can be expressed as the convolution with the step responses at the impacted tips, as

$$\begin{aligned} U(t) &= \int_0^t \frac{F\left(t-t'\right)}{A}\frac{d}{dt'}\left(\frac{u\left(0,t'\right)}{\sigma_0}\right)dt', \\ U_I(t) &= \int_0^t \frac{F\left(t-t'\right)}{A}\frac{d}{dt'}\left(\frac{u_I\left(0,t'\right)}{\sigma_0}\right)dt', \end{aligned} \tag{5}$$

where $F(t)$ and A are impact force due to the collision and cross-sectional areas of both bars. $u(x,t)$ and $u_I(x',t)$ are the displacements of the FGM bar and the impact bar subjected to step force per unit cross-sectional area, σ_0, which are solved in Sect. 2.3.

2.2 Step Response of FGM Bar

The response of the FGM bar is subjected to step force per unit cross-sectional area, $\sigma_0 H(t)$ at the tip $x = 0$. The other end $x = L$ of the bar is fixed.

$$\sigma = -\sigma_0 H(t) \text{ at } x = 0 \text{ and } u = 0 \text{ at } x = L, \tag{6}$$

where $H(t)$ is Heaviside step function. The initial condition is

$$u = \partial u/\partial t = 0 \text{ at } t = 0. \tag{7}$$

The equilibrium of stress for the FGM bar is given as

$$\frac{\partial \sigma(x,t)}{\partial x} = \rho(x) \frac{\partial^2 u(x,t)}{\partial t^2}. \tag{8}$$

By using Laplace transformation, Eq. (8), the solution can be reduced.

$$\frac{E_0}{\sigma_0 L} \bar{u}(\xi, s) = -\frac{1}{\Phi_1^2 \Phi_0^3 s} \frac{\left(\frac{\xi+\Phi_0}{1+\Phi_0}\right)^{\lambda_1} - \left(\frac{\xi+\Phi_0}{1+\Phi_0}\right)^{\lambda_2}}{\lambda_1 \left(\frac{\Phi_0}{1+\Phi_0}\right)^{\lambda_1} - \lambda_2 \left(\frac{\Phi_0}{1+\Phi_0}\right)^{\lambda_2}}, \tag{9}$$

where

$$\lambda_{1,2} = -\frac{3}{2} \pm \frac{\sqrt{9\Phi_1^2 + 4\Phi_1 s^2}}{2\Phi_1}, \ \xi = \frac{x}{L}.$$

The Laplace transformation is defined as

$$\bar{u}(s) = \int_0^\infty u(\tau) \exp(-s\tau) \, d\tau, \ \tau = \frac{C_0}{L} t, \quad C_0^2 = \frac{E_0}{\rho_0}.$$

2.3 Analytical Procedure

By substituting Eq. (9) into Laplace transformed Eqs. (4) and (5), the impact force in Laplace transformed domain can be derived. The impact force is inversed numerically from the Laplace transformed domain to the time domain by using the numerical inversion of the Laplace transformation described in Sect. 2.4. The calculated impact force will increase compressively just after the collision and change to tension owing to the return of the reflected wave to the collision point after complicated fluctuation. However, the impact force must be definitely compressive because the tips of the impactor solely contact at the tip of the FGM bar and are not joined. The bars separate mutually just when the impact force transforms from the compression to the tension. Therefore, the calculated impact force after the force changes to the tension should become zero to express the termination of the

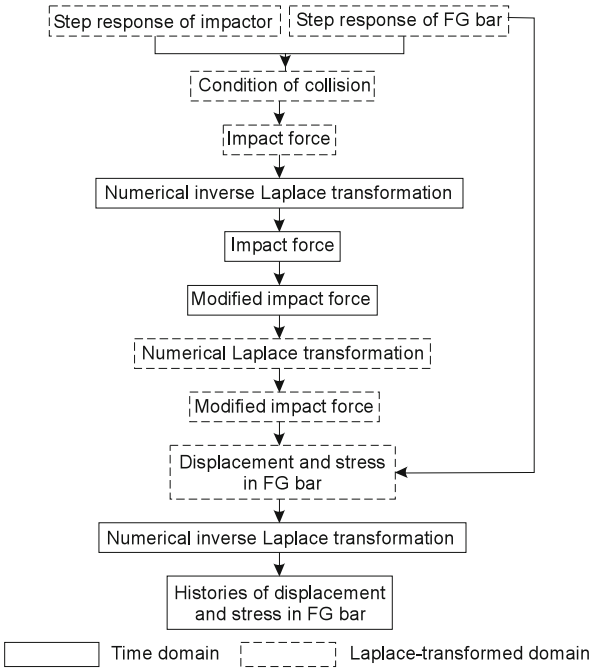

Fig. 2 Computational flow

collision. The impact force $F(t)$ calculated with Eq. (4) and the numerical inversion of the Laplace transformation are redefined as the modified impact force $F_C(t)$ as follows:

$$F_C(t) = \begin{cases} F(t) & t \leq t_c \\ 0 & t > t_c \end{cases}, \tag{10}$$

where t_c is the first time that impact force $F(t)$ turns to tension.

After the impact force $F_C(t)$ is Laplace transformed again, the transformed load is substituted into Eqs. (3) and (9) to clarify the stress histories in the FGM bar. The computational flow of the analysis is summarized in Fig. 2.

2.4 Numerical Laplace Transformation

The numerical Laplace transformation is formulated on the basis of Krings-Waller's numerical inversion [20, 21] to calculate the analyzed solutions. The pair of numerical Laplace transformation on the basis of Krings-Waller's method can be formulated as follows [22]:

$$\bar{u}\left(\gamma + in \cdot \Delta\omega\right) = \frac{T}{N}\sum_{k=0}^{N-1} u\left(k \cdot \Delta\tau\right)\exp\left(-\gamma k \cdot \Delta\tau\right)\exp\left(-\frac{i2\pi nk}{N}\right)$$

$$u\left(k \cdot \Delta\tau\right) = \frac{\exp\left(\gamma k \cdot \Delta\tau\right)}{T}\sum_{n=0}^{N-1} \bar{u}\left(\gamma + in \cdot \Delta\omega\right)\exp\left(\frac{i2\pi nk}{N}\right). \tag{11}$$

In Eq. (11), γ is greater than the real part of all singularities of Laplace transformed $u(t)$. The parameter s is discretized into N parts along the integration path with consideration for the sampling theorem in Fourier transformation.

$$s = \gamma + i \cdot n\Delta\omega,\ n = 0,\ 1,\ 2,\ \cdots,\ N-1, \tag{12}$$

where

$$\Delta\omega = 2\pi \Big/ T, \quad i = \sqrt{-1}, \quad \Delta\tau = \frac{T}{N}. \tag{13}$$

T is time range in the calculation.

In actual numerical calculation, N and γ parameters are determined in consideration of the accuracy of results with analyzed time duration T. The actual values of the parameters are determined as $N = 2^{14}$ and $\gamma = 8/T$ for accuracy. Numerical results calculated by Eq. (11) fluctuate dramatically with time and this accuracy decreases in the later analyzed time duration. Therefore in order to ensure necessary accuracy, the results in the latter quarter of the analyzed time are eliminated [21].

3 Numerical Results

We analyzed numerically wave propagations in two FGM bars. One FGM bar (FGM bar A) had Young's modulus distributed increasing from the impact end to the one fixed end (Young's modulus, $E(L)/E(0) = 10$) and the other bar (FGM bar B) had the modulus distributed decreasingly (Young's modulus, $E(L)/E(0) = 0.1$). Therefore, the boundary condition of the FGM bar B inverts the impact end and fixed end of the FGM bar A. The lengths of the FGM bars were the same as the one of the impact bar.

Figure 3 shows stress history at each position of the FGM bar A having the Young's modulus distributed increasingly from the impact end. The history at the impact end ($x/L = 0$) denotes impact load history due to the collision. The histories vary more steeply at more close position of the FGM bar. The history at the fixed end fluctuated intensively. Generally when the impact bar collided to a homogeneous bar with the same boundary condition, stress is compressive at any position of the bar [23]. However in this case large tensile stress generates by stress wave reflected at the fixed end. Figure 4 shows stress history at each position of the FGM bar B having the Young's modulus distributed decreasingly from the impact end. The histories

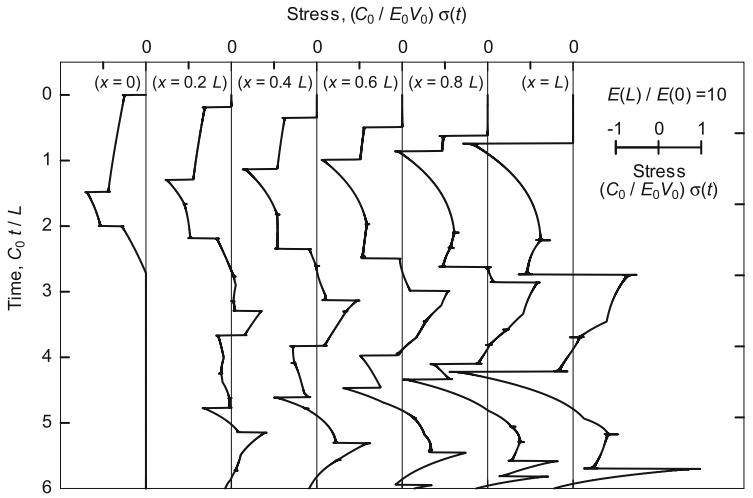

Fig. 3 Stress histories in FGM bar A. Horizontal axis denotes amplitude of stress at each point. $L/L_I = 1.0$

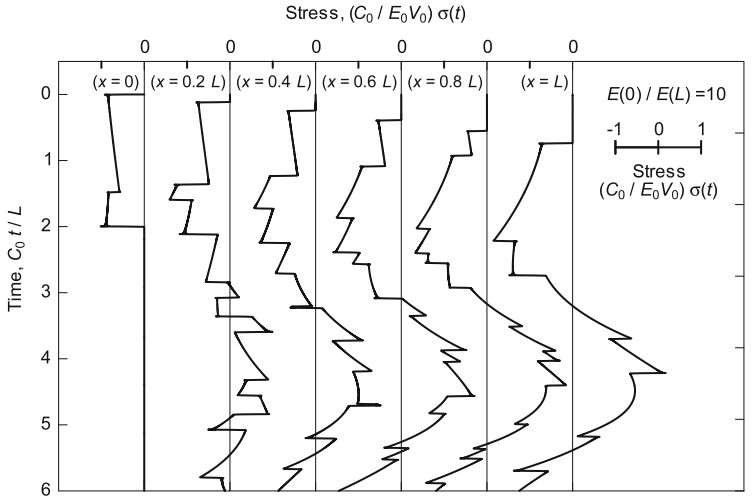

Fig. 4 Stress histories in FGM bar B. Horizontal axis denotes amplitude of stress at each point. $L/LI = 1.0$

varied smoothly with small steps and could be approximated by a sine curve. The histories had much different trends from the ones of the bar A.

Finally the stress histories in the FGM bar collided by the impact bar are much different from the histories for collisions to a homogeneous bars [23] and are found to be strongly dependent on the distribution of mechanical properties: density and Young's modulus. When we apply the FGM to mechanical components for impact

energy absorption, slope of the mechanical properties in the component must be considered.

4 Conclusion

Wave propagations in the FGM bars collided by a homogeneous bar were analyzed on the basis of Laplace transformation and were calculated by using numerical transformation and its inversion. Finally in the FGM bar with increasing modulus from the impact end to the fixed end, much larger compressive stress and even large tensile stress occurred near the fixed end. In the FGM bar with decreasing modulus from the impact end, the compressive stress was approximately the same as the one in the homogeneous bar, and the history of the stress varied moderately however large tensile stress occurred.

References

1. Tanigawa, Y.: Some basic thermoelastic problems for nonhomogeneous structural materials. Appl. Mech. Rev. **48**, 287–300 (1995)
2. Noda, N.: Thermal stresses in functionally graded material. J. Therm. Stress. **22**, 377–512 (1999)
3. Adachi, T., Higuchi, M.: Development of integral molding of functionally-graded syntactic foams. In: Irschik, H., Krommer, M., Belyaev, A.K. (eds.) Advanced Dynamic and Model-Based Control of Structures and Machines, pp. 1–9. Springer, Heidelberg (2012)
4. Higuchi, M., Adachi, T., Yokochi, Y., Fujimoto, K.: Controlling of distribution of mechanical properties in functionally-graded syntactic foams for impact energy absorption. Mater. Sci. Forum **706–709**, 729–734 (2012)
5. Adachi, T., Higuchi, M.: Fabrication of bulk functionally-graded syntactic foams for impact energy absorption. Mater. Sci. Forum **706–709**, 711–716 (2012)
6. Cui, L., Kiernan, S., Gilchrist, M.D.: Designing the energy absorption capacity of functionally graded foam materials. Mater. Sci. Eng. A **507**, 215–225 (2009)
7. Chiu, T.C., Erdogan, F.: One-dimensional wave propagation in a functionally graded elastic medium. J. Sound Vib. **222**, 453–487 (1999)
8. Bruck, H.A.: One-dimensional model for designing functionally graded materials to manage stress waves. Int. J. Solids Struct. **37**, 6383–6395 (2000)
9. Abu-Alshaikh, I., Kokluce, B.: One-dimensional transient dynamic response in functionally graded layered media. J. Eng. Math. **54**, 17–30 (2006)
10. Kiernan, S., Cui, L., Gilchrist, M.D.: Propagation of a stress wave through a virtual functionally graded foam. Int. J. Non-Linear Mech. **44**, 456–468 (2009)
11. Han, X., Liu, G.R., Lam, K.Y., Ohyoshi, T.: A quadratic layer element for analyzing stress waves in FGMs and its application in material characterization. J. Sound Vib. **236**, 307–321 (2000)
12. Santare, M.H., Thamburaj, P., Gazonas, G.A.: The use of graded finite elements in the study of elastic wave propagation in continuously nonhomogeneous materials. Int. J. Solids Struct. **40**, 5621–5634 (2003)
13. Samadhiya, R., Mukherjee, A., Schmauder, S.: Characterization of discretely graded materials using acoustic wave propagation. Comput. Mater. Sci. **37**, 20–28 (2006)

14. Berezovski, A., Engelbrecht, J., Maugin, G.A.: Numerical simulation of two-dimensional wave propagation in functionally graded materials. Eur. J. Mech. A-Solids **22**, 257–265 (2003)
15. Liu, G.R., Han, X., Xu, Y.G., Lam, K.Y.: Material characterization of functionally graded material by means of elastic waves and a progressive-learning neural network. Compos. Sci. Technol. **61**, 1401–1411 (2001)
16. Adachi, T., Yoshigaki, N., Higuchi, M.: Analysis of longitudinal impact problem for functionally graded materials. Trans. Jpn. Soc. Mech. Eng. A **79**, 502–510 (2012)
17. Higuchi, M., Yokochi, Y., Adachi, T.: Evaluation on integrated molding of functionally-graded epoxy foams. Trans. Jpn. Soc. Mech. Eng. A **78**, 660–664 (2012)
18. Higuchi, M., Adachi, T., Yoshioka, T., Yokochi, Y.: Evaluation on distributions of mechanical properties in functionally graded syntactic foam. Trans. Jpn. Soc. Mech. Eng. A **78**, 890–901 (2012)
19. Adachi, T., Higuchi, M.: Impulsive responses of functionally graded material bars due to collision. Acta Mech. **224**, 1061–1076 (2013)
20. Krings, W., Waller, H.: Contribution to the numerical treatment of partial differential equations with the Laplace transformation – an application of the algorithm of the fast Fourier transformation. Int. J. Numer. Methods Eng. **14**, 1183–1196 (1979)
21. Adachi, T., Ujihashi, S., Matsumoto, H.: Impulsive responses of a circular cylindrical shell subjected to waterhammer waves. J. Press. Vessel Technol. **113**, 517–523 (1991)
22. Adachi, T., Sakanoue, K., Ujihashi, S., Matsumoto, H.: Damage evaluation of CFRP laminates due to iterative impact. Trans. Jpn. Soc. Mech. Eng. A **57**, 569–575 (1991)
23. Graff, K.: Wave Motion in Elastic Solids. Dover, New York (1991)